X-611-68-119
PREPRINT

NASA TM X- 63195

A SOLID STATE DETECTOR EXPERIMENT FOR ELECTRON MEASUREMENTS ON OGO-F

JAMES H. TRAINOR
DONALD J. WILLIAMS

GPO PRICE $ _____

CFSTI PRICE(S) $ _____

Hard copy (HC) 3.00

Microfiche (MF) .65

ff 653 July 65

GSFC
GODDARD SPACE FLIGHT CENTER
GREENBELT, MARYLAND

N68-22703

FACILITY FORM 602

(ACCESSION NUMBER) (THRU)

16 1

(PAGES) (CODE)

TMX-63195 14

(NASA CR OR TMX OR AD NUMBER) (CATEGORY)

MAY 1968
RECEIVED
NASA STI FACILITY
INPUT BRANCH

X-611-68-119

A SOLID STATE DETECTOR EXPERIMENT FOR ELECTRON MEASUREMENTS ON OGO-F

James H. Trainor
and
Donald J. Williams

GODDARD SPACE FLIGHT CENTER
Greenbelt, Maryland

PRECEDING PAGE BLANK NOT FILMED.

A SOLID STATE DETECTOR EXPERIMENT FOR ELECTRON MEASUREMENTS ON OGO-F

James H. Trainor
Donald J. Williams

SUMMARY

A solid state detector system is described which has been developed for flight on an Orbiting Geophysical Observatory in polar orbit. Measurements will be made of the electron flux and spectra above 35 KeV, both for precipitating and locally mirroring electrons, as well as atmospheric backscatter.

This paper reviews the physical need and the design requirements of such an experiment; and describes the detector and electronic implementation of the experiment including the methods of monitoring detector and electronic performance in flight.

PRECEDING PAGE BLANK NOT FILMED.

CONTENTS

	Page
SUMMARY	iii
INTRODUCTION	1
THE DETECTORS	1
THE SPACECRAFT SYSTEM	3
CALIBRATION	4
CONCLUDING REMARKS	5
REFERENCES	5

A SOLID STATE DETECTOR EXPERIMENT FOR ELECTRON MEASUREMENTS ON OGO-F

INTRODUCTION

This experiment measures the intensities of trapped, precipitated, and backscattered electrons in the integral energy ranges, $E_e \geqslant 35$ KeV, $\geqslant 100$ Kev, $\geqslant 300$ Kev, and $\geqslant 1.0$ MeV. The main goal of the experiment is to obtain and study the spatial distributions and time histories of these low altitude outer zone electrons.

Such studies have yielded quantitative results on the adiabatic motion of trapped electrons in the distorted geomagnetic field[1] and in a distorted geomagnetic field including electric field effects.[2] In addition, the relation and interplay of the outer zone with the geomagnetic tail and with perturbations in the solar wind have been studied utilizing similar low altitude data.[3,4] Studies of electron precipitation[5,6] have led to an increased understanding of the nature of the loss mechanisms occurring in the outer zone.[7]

Continuing these studies on the OGO-F satellite offers the opportunity of observing these phenomena during the period of maximum solar activity, a period which should be characterized by enhanced magnetic activity in the magnetosphere. The nearly polar, low altitude orbit of OGO-F offers a high sampling density of all outer zone field lines; a relatively stable local field configuration and consequent knowledge of which field line is being sampled; and a large loss cone, making it a simple matter to sample precipitated electron intensities.

THE DETECTORS

The detection method utilized in this experiment is simply to monitor the amplified output of a totally depleted 500μ surface barrier solid state detector with two discriminator levels. These detectors totally deplete at ~120 volts and are operated at a full bias of 150 volts. The lower of the two discriminator levels, together with detector shielding, determines the low energy threshold of the unit. The higher level is included to reduce possible proton contamination effects.

The operation is illustrated in Figure 1 where we show the average electron energy loss[8] in 500μ of silicon as a function of incident electron energy. This thickness detector corresponds to a 10% transmission range of ~411 KeV electrons. An upper discriminator level of 750 KeV and a lower level of 100 KeV

are shown. It is seen from the average energy loss values shown in Figure 1 that all electrons $\geqslant$100 KeV will be detected. The proton sensitivity will be confined to 100 KeV $\leqslant E_p \leqslant$ 750 KeV and $E_p \gtrsim$ 88 Mev. Note that with no upper level the proton sensitivity increases to $E_p \gtrsim$ 100 KeV. In light of proton spectra observed in the trapping regions, the inclusion of an upper level yields significant proton discrimination. In fact it has been shown that such proton contamination is negligible at low altitudes.[9]

It is important to consider the effects of path length and energy straggling when detecting electrons. For example, the actual setting of the upper discriminator level (750 KeV) was chosen as a compromise between maintaining high detection efficiency for $\geqslant$750 KeV electrons and simultaneously obtaining a low proton sensitivity. The lower level of an integral detector must also be set to provide a high detection efficiency of minimum ionizing electrons. While the average energy loss of a 1.5 Mev electron in 500μ of Si is $\sim$230 KeV, the most probable energy loss is $\sim$150 KeV and the FWHM of the Landau distribution is $\sim$48 KeV. To detect $\gtrsim$ 96% of these minimum ionizing electrons (excluding backscatter and edge effects) the lower discriminator should be at least 2σ below the most probable energy loss. For the 500μ detectors considered here, this yields a lower level of 150-41 = 109 KeV and shows that a 100 KeV is satisfactory.

Table 1 shows the discriminator levels, shielding thicknesses and final particle sensitivities for the experiment. The lower levels shown at 35 KeV are commandable to 75 KeV via ground command in case of detector failure or excessive noise. The 12.5μ inch Ni foil is used for light and heat shielding purposes.

Figure 2 shows a mechanical cross-section of a detector assembly. (1) and (2) refer to the body shield and snout of the assembly which are made of Cu with a Pb liner (3). A Kel-F liner (7) provides electrical isolation. The transmission detector is mounted in a ceramic ring (12), mechanically buffered with wire washers (4) which also pick up the electrical contact. Bias and signal connections to the detector are made through a washer (6) which is soldered to a pin extending into one side of a Microdot 53-121 adapter (5). The 50-ohm side screws into the mount, and the 93-ohm side is used for the external cable connection.

Also shown is the assembly of a GaAs photoluminescent diode (11) into the mount. The diode is held in place by a Kel-F sleeve (10) which also provides insulation for the welded pigtail bringing the signal to the diode. The entire assembly is held firmly in place by the hollow screw (8) and ferrule (9).

Detection efficiency vs incident electron energy for a 500μ, totally depleted detector is shown in Figure 3. This detector has a 12.5μ inch Ni window and electronic thresholds at 100 KeV and somewhat under 750 KeV. Approaching the

upper threshold, one can see that a few percent of the electrons deposit a very large fraction of their energy in the detector and are rejected. As expected, this is less of an effect at higher energies. With the typical electron spectra of physical concern here, the average efficiency for the detector would be ~90-94%.

THE SPACECRAFT SYSTEM

The OGO is a three-axis controlled spacecraft, which in the case of OGO-F, will be put into a near-Earth, polar orbit. One side of the spacecraft (+Z) is constrained to always point toward the center of the Earth under the direction of infrared horizon sensors. Sun sensors then direct rotation about the Z axis in order to maximize the electrical power output from the solar arrays and allow solar-pointing experiments. An additional result is that three faces on the spacecraft and its appendages (+X, -X and +Y) never see the sun directly. The main body of the spacecraft mounts thermal control louvers on the X faces.

This experiment is mounted on the EP-2 experiment boom and uses the +Y face of the experiment package as a radiating surface to dump heat from the experiment. With multiple layer insulation around the rest of experiment, and less than 2 watts electrical dissipation, the experiment will run at approximately -20°C in flight. In doing this, the system noise is reduced by ~25% compared with ambient temperatures. The limitation here is the performance of our low power, wide temperature range, charge sensitive preamplifiers, however, this reduction in noise significantly increases the low noise lifetime of the experiment.

Figure 4 shows the orientation of the detector assemblies with respect to the radius vector to the center of the Earth (+Z). In our region of interest—i.e., at low altitudes and invarient geomagnetic latitudes $\gtrsim 60°$—the inclinations of the field lines are greater than 78°. This then guarantees that detectors 5 and 6 with their 30° entrance cones are aligned to monitor precipitating particles. Similarly, detector 7 will monitor atmospheric backscatter or albedo, and detectors 1 through 4 with their 15° entrance cones will be aligned to within 12° of the local field direction and will monitor trapped particles mirroring at or very near the point of observation.

Finally, Figure 4 also indicates that the data from the seven integral detectors are commutated into 4 quasi-logarithmic counters such that, alternately, data is recorded from detectors 1, 2, 3 and 4 and then 1, 5, 6 and 7. While one set of data is being taken, the other is being read from shift register into the spacecraft, etc. Additionally, on a low duty cycle we monitor the rates from the upper level thresholds in order to put together a crude proton and heavy particle spectra, if indeed they are present. The system performance is such that

the maximum uncertainty in the gain of the preamplifier - amplifier - discriminator system is ±4% over the temperature range of -40°C to +40°C.

CALIBRATION

In flight, the experiment will go over to a calibrate mode every 80 minutes whereby known charge pulses are applied to the inputs of all the charge preamplifiers. The amplitude of these charge pulses is systematically decreased in 10 KeV steps from 810 to 700 KeV and from 130 to 20 KeV, bracketing and checking all discriminator levels. Figure 5 shows the result of pulse height analysis through the experiment electronics of the 130 to 40 KeV pulses. The electronic noise performance of the system is ~5 KeV.

Since the spacecraft data clock is used to set the pulse rate, an easily recognizable number results regardless of the spacecraft bit rate. Additionally, we apply a 420 KHz signal for 32 frames in each calibration sequence to check on the experiment's high count rate capability and the compression.

Previously GaAs photoluminescent diodes were shown included in each detector assembly. The intent is to be able to stimulate the detectors directly, allowing a pulsed calibration scheme whereby the discriminators are bracketed again with known energy pulses, each energy step having a characteristic pulse rate. The intent is to be able to separate detector and electronic effects.

Figure 6 shows the equivalent particle-energy-effect of the GaAs light flashers as a function of temperature. The nominal energies noted for each curve are for 23°C. There is a large effect with temperature; the slope is different in different energy regions. Additionally, different detectors respond differently to the same light. Our approach is to pair off a given photoluminescent diode with a detector and housing; calibrate them as shown here; then use a computer to select the type of network and component values necessary to compensate the temperature effect. It appears that we have been able to accomplish this flattening to ±10% in our region of interest. We are just now evaluating the long term performance.

Complementing the pulsed calibration modes, the experiment also measures all detector leakage currents, detector biases, temperature at several locations; has the ability to select detector bias voltages by command; and can change from 35 KeV to 75 KeV discriminators on the low energy channels should there be measurable noise due to radiation damage, thermal effects, etc.

CONCLUDING REMARKS

A similar although less grand unit employing five 1000μ surface barrier detectors was flown aboard the polar orbiting satellite 1963 38C by D. J. Williams and C. O. Bostrom.[9] That unit is still operating very satisfactorily 4-1/2 years after launch. The present experiment should assure continuing data through the next solar maximum, as well as data on the aging of the system. The latter data are necessary for the continuing design of very long life experiments required for long, deep space missions.

REFERENCES

1. D. J. Williams and G. D. Mead, "A Nightside Magnetospheric Configuration as Obtained from Trapped Electrons at 1100 Kilometers," J. Geophys. Res., 70, 3017, (1965)

2. H. E. Taylor, "Adiabatic Motion of Outer Zone Particles in a Model of the Geoelectric and Geomagnetic Fields," J. Geophys. Res., 71, 5135, (1966)

3. D. J. Williams, "A 27-Day Periodicity in Outer Zone Trapped Electron Intensities," J. Geophys. Res., 71, 1815, (1966)

4. D. J. Williams and N. F. Ness, "Simultaneous Trapped Electron and Magnetic Tail Field Observations," J. Geophys. Res., 71, 5117, (1966)

5. B. J. O'Brien, "High Latitude Geophysical Studies with Satellite INJUN 3, 3: Precipitation of Electrons into the Atmosphere," J. Geophys. Res., 69, 13, (1964)

6. I. B. McDiarmid and J. R. Burrows, "Diurnal Intensity Variations in the Outer Radiation Zone at 1000 Km," Can. J. Phys., 42, 1135, (1964)

7. C. F. Kennel and H. E. Petschek, "Limit on Stably Trapped Particles," J. Geophys. Res., 71, 1, (1966)

8. L. Katz and A. S. Penfold, "Range-Energy Relations for Electrons and the Determination of Beta-Ray End-Point Energies by Absorption," Rev. Mod. Phys., 24, 28, (1952)

9. D. J. Williams and A. M. Smith, "Daytime Trapped Electron Intensities at High Latitudes at 1100 Kilometers," J. Geophys. Res., 70, 541, (1965)

FIGURE CAPTIONS

Figure 1. Average $\triangle E$ vs E for electrons in 500μ silicon.

Figure 2. Cross-section of a detector assembly.

Figure 3. Detection efficiency vs incident electrons energy.

Figure 4. Detector orientation and data pattern.

Figure 5. Pulse height analysis of the 130 KeV to 40 KeV calibration signals.

Figure 6. Temperature effects of a GaAs photoluminescent diodes.

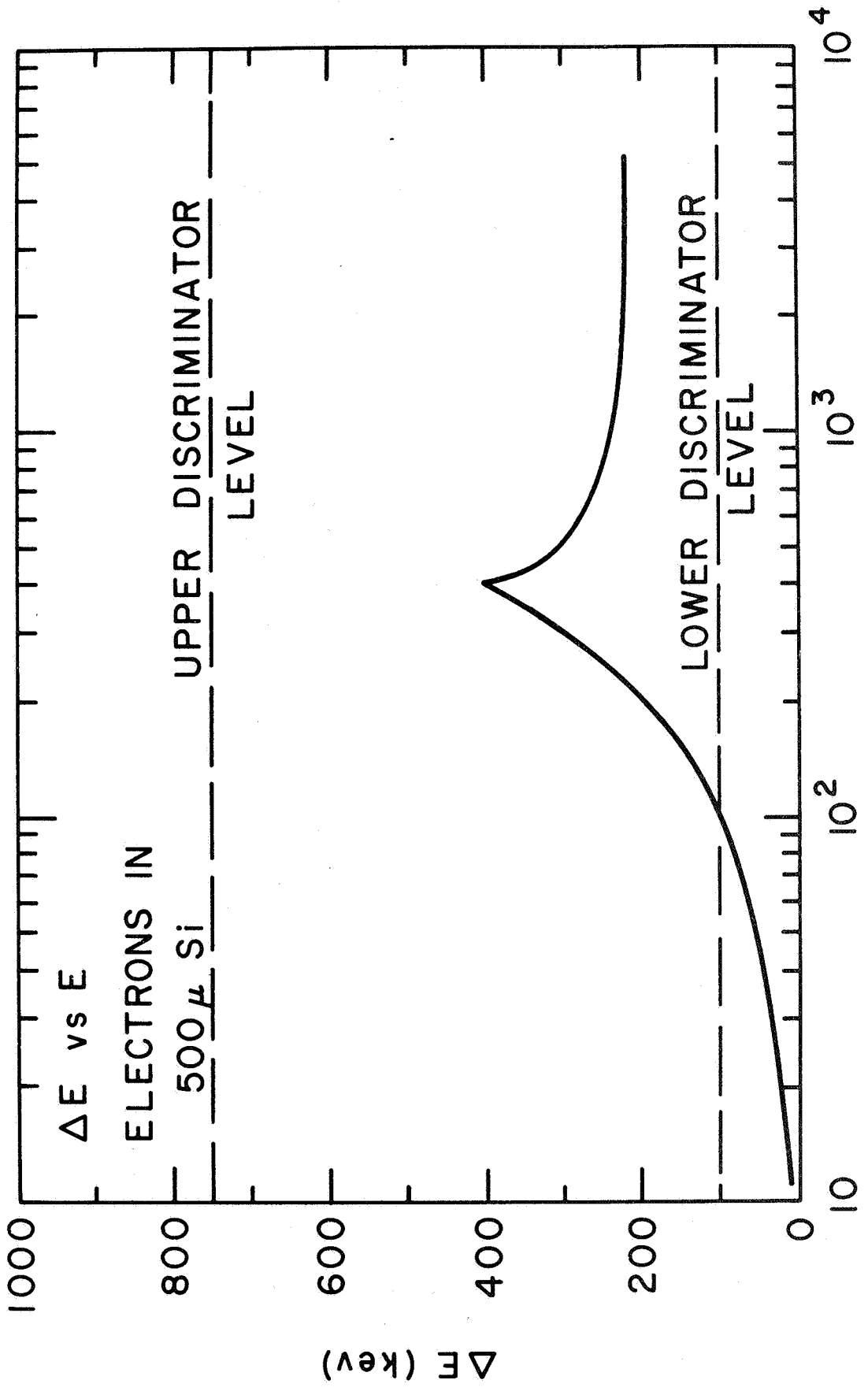
ΔE vs E
ELECTRONS IN
500 μ Si
UPPER DISCRIMINATOR
LEVEL
LOWER DISCRIMINATOR
LEVEL
ΔE (kev)
E_i (kev)
1000
800
600
400
200
0
10
10^2
10^3
10^4

Figure 1

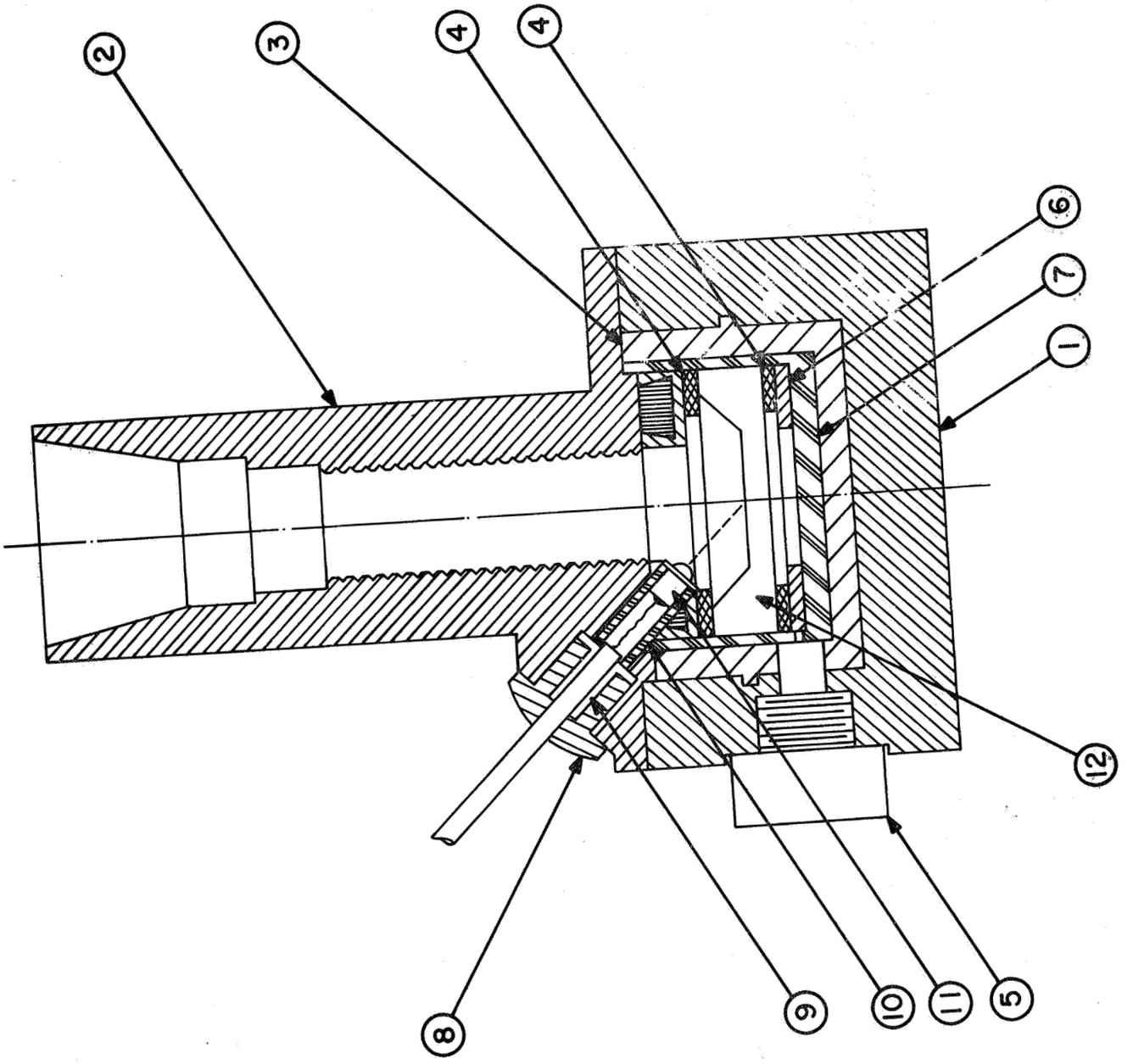

Figure 2

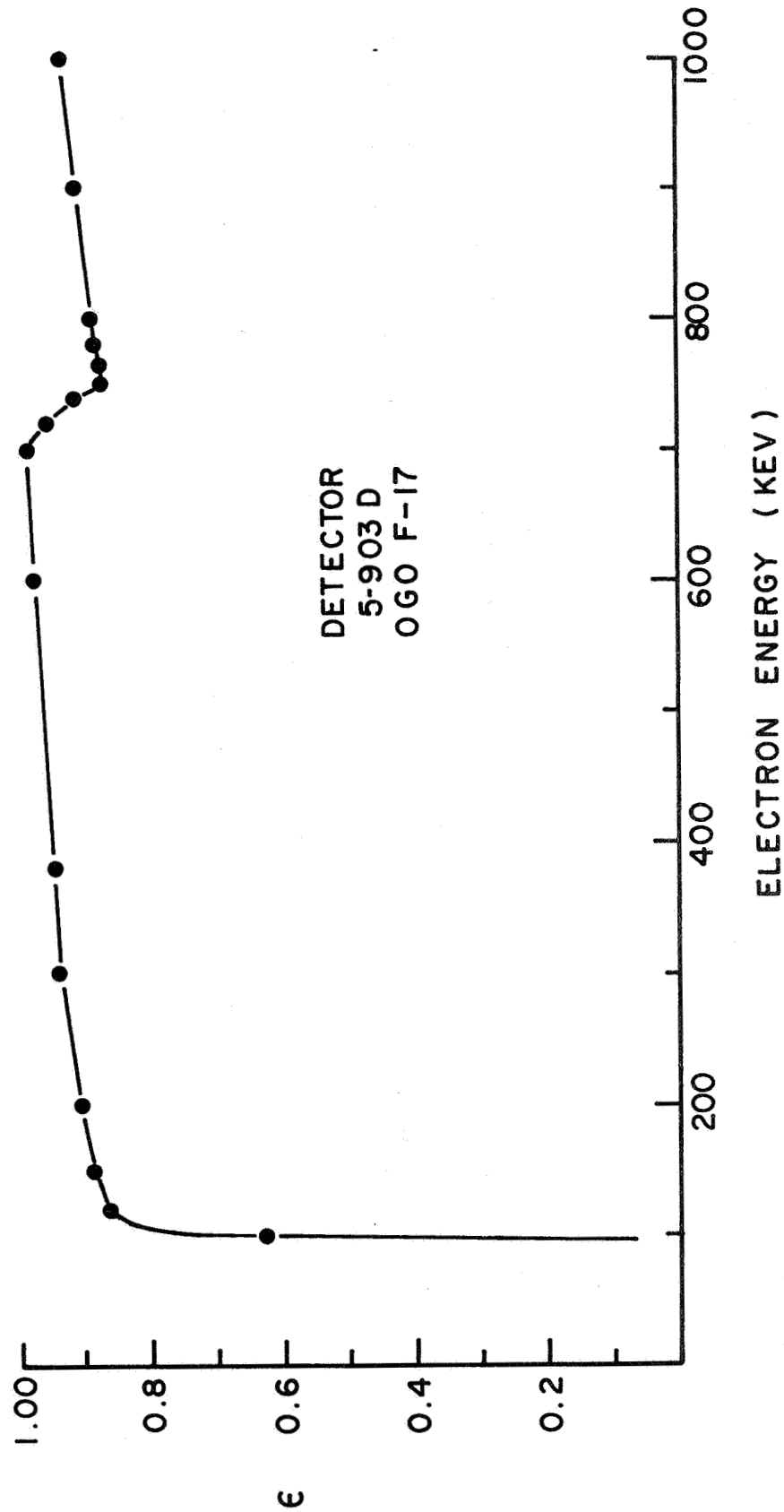
DETECTOR
5-903 D
OGO F-17
ε
1.00
0.8
0.6
0.4
0.2
200
400
600
800
1000
ELECTRON ENERGY (KEV)

Figure 3

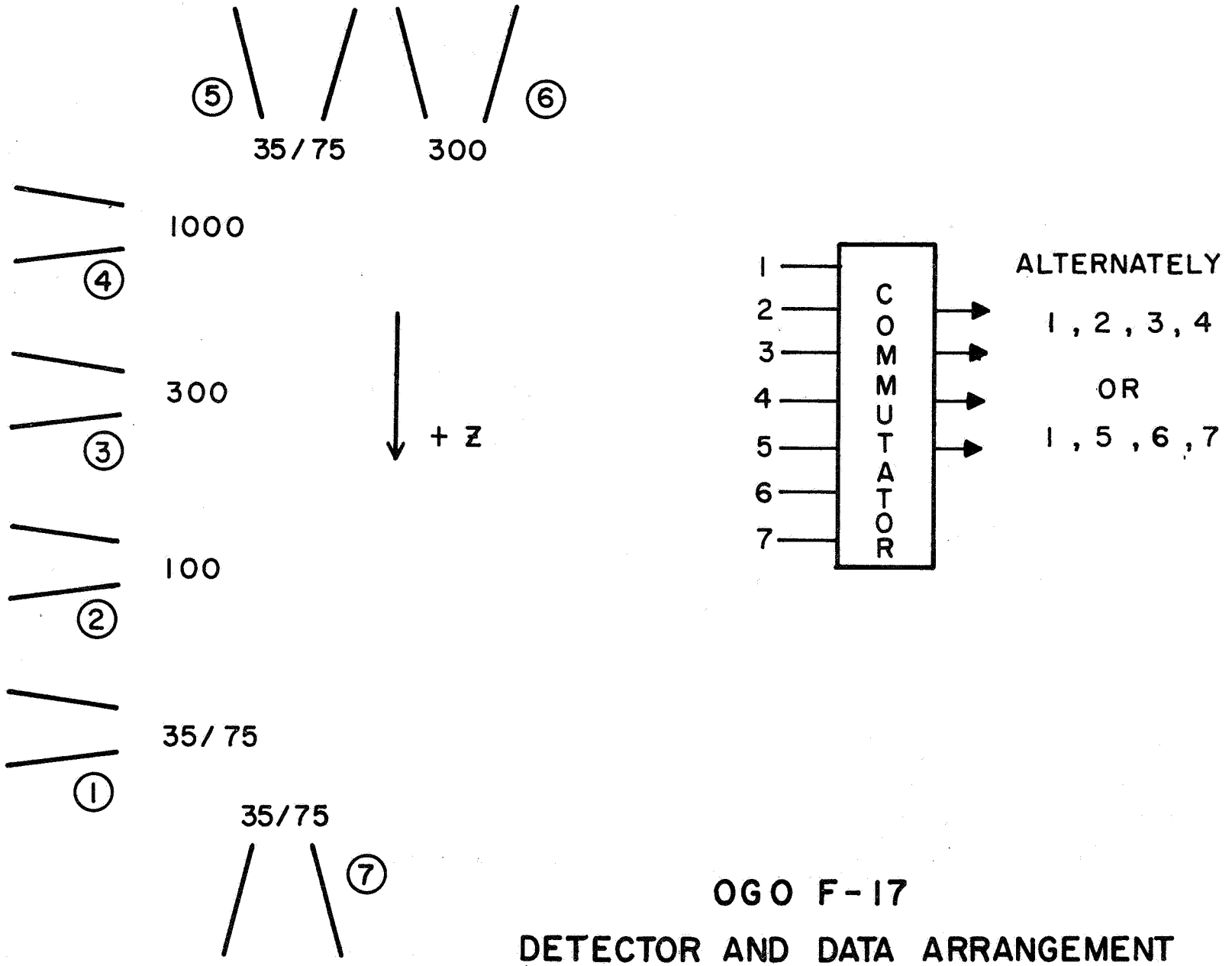

OGO F-17

DETECTOR AND DATA ARRANGEMENT

Figure 4

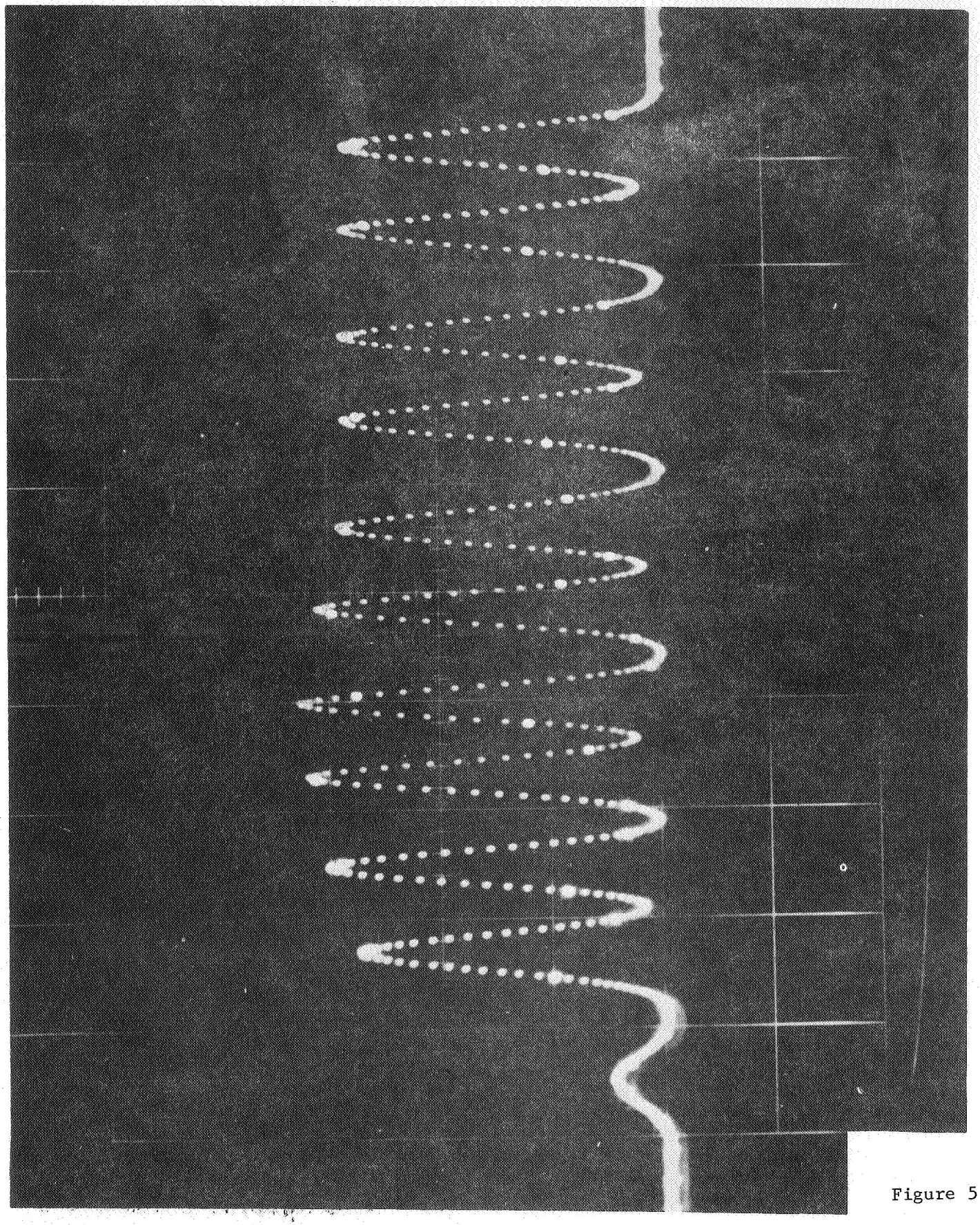

Figure 5

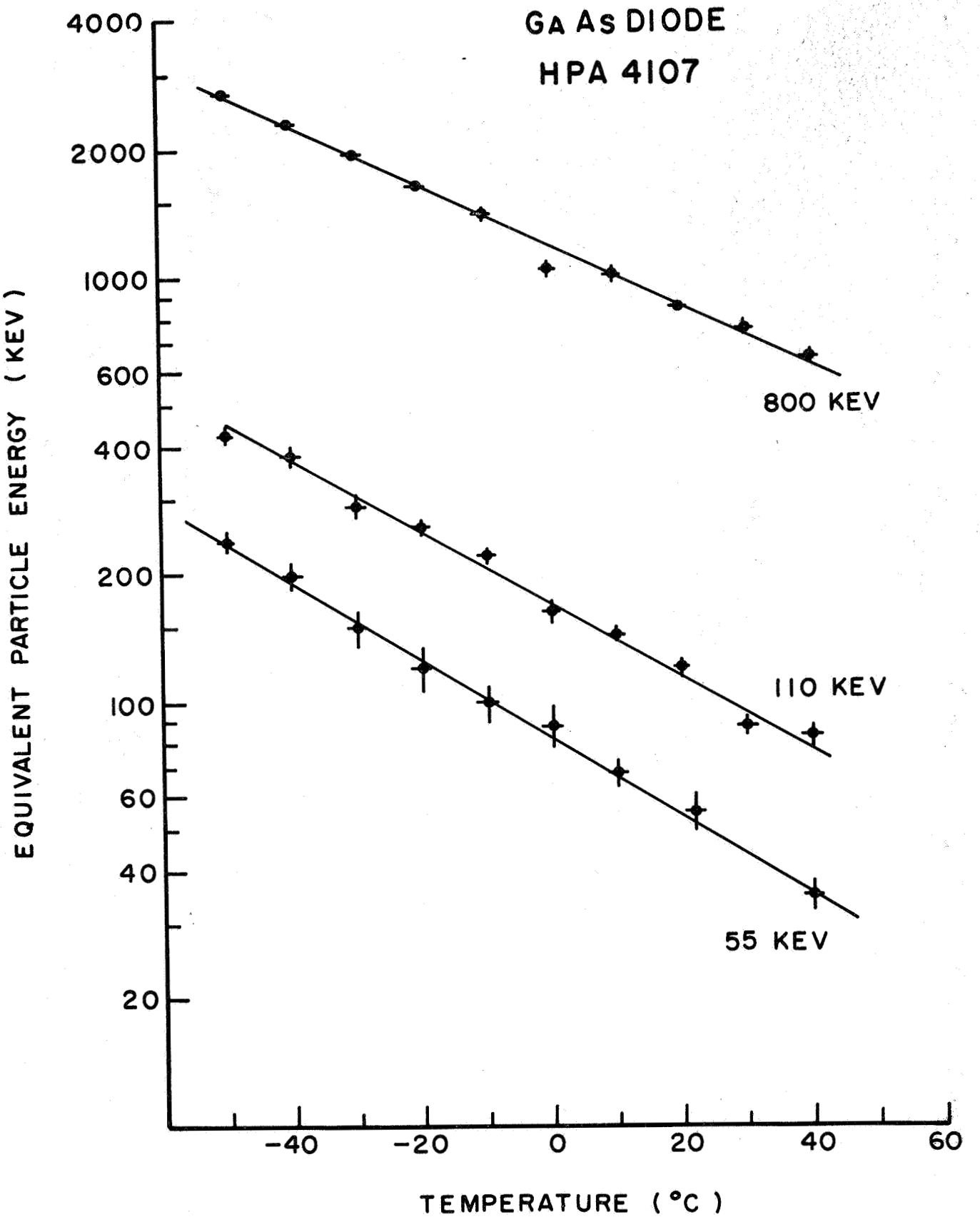
GA AS DIODE
HPA 4107
4000
2000
1000
600
400
200
100
60
40
20
800 KEV
110 KEV
55 KEV
EQUIVALENT PARTICLE ENERGY (KEV)
-40
-20
0
20
40
60
TEMPERATURE (°C)

Figure 6